JOURNAL OF SPACECRAFT AND ROCKETS
Vol. 32, No. 1, January–February 1995

Hammerhead and Nose-Cylinder-Flare Aeroelastic Stability Revisited

J. Peter Reding* and Lars E. Ericsson†
Lockheed Missiles and Space Company, Sunnyvale, California 94086

The flow mechanism responsible for the recently discovered buffet-producing critical cylinder length for hammerheads is discussed. For short cylinder lengths, the upstream effects of the hammerhead wake are able to affect the terminal shock location, driving flow separation to the nose-cylinder shoulder. This has the potential to cause aeroelastic instability leading to structural failure. A similar critical-cylinder-length effect exists for cone-cylinder-flare configurations. This too involves an upstream flow effect. In this case the flare-induced pressure rise drives the shock-induced flow separation to the cone-cylinder shoulder. Neither of these effects is recognized in the existing NASA guidelines for elastic vehicle design. Some currently proposed designs for heavy lift launch vehicles incorporate dangerously blunt noses, in violation of the NASA aeroelastic design criterion. A reexamination of these nose effects indicates the possibility of aeroelastic instability and structural failure. It is the conclusion of this study that it is imperative to consider aeroelastic stability effects early in the design process in order to avoid the possibility of a flight failure or a costly redesign later in the development cycle if the presence of an aeroelastic stability problem is discovered.

Nomenclature

A	= reference area, $\pi D^2/4$, ft^2
C_σ	= buffet coefficient, σ/qAD
C_p	= pressure coefficient, $C_p = (p - p_\infty)/q_\infty$
D, d_N	= payload diameter, ft
d	= booster diameter, ft
L, L_n	= length parameters (Fig. 4), ft
L_N	= hammerhead length (Fig. 1), ft
M	= Mach number
p	= static pressure, psf
q_∞	= dynamic pressure, $\rho_\infty U_\infty^2/2$, psf
U	= velocity, ft/s
x	= axial coordinate, ft
z	= dimensionless modal deflection coordinate (Fig. 2)
α	= angle of attack, deg
θ_c	= nose-cone angle, deg
ρ	= air density, lb-s^2/ft^4
ξ	= dimensionless x coordinate, x/d (Fig. 6)
σ	= root-mean-square bending moment, ft-lb

Subscripts

crit	= critical condition
∞	= freestream conditions

Introduction

CURRENT needs for heavy launch capability have renewed interest in large, nonrecoverable space boosters. This, along with the advantage of using a well-tested, reliable, "bus" as a workhorse booster for a variety of arbitrary, or as yet undefined, payloads has caused designers to renew their interest in hammerhead configurations. This has resulted in analytical and experimental investigations of hammerhead payload shrouds with an eye toward understanding their aeroelastic stability problems.[1–5] In addition to the flow separation on the hammerhead boattail, the flow separation occurring on the nose-cylinder shoulder of the payload can often be cause for concern, alone as well as in combination with a hammerhead or a flare.[6]

Received June 22, 1993; revision received June 15, 1994; accepted for publication June 20, 1994.

*Retired; gentleman of leisure. Associate Fellow AIAA.
†Retired; engineering consultant. Fellow AIAA.

In recent tests[7] of the hammerhead geometry shown in Fig. 1, the response of a partial simulation of the second bending mode (Fig. 2) was benign except for the case when $L_N/d_N = 0.3$ (Fig. 3). This critical-cylinder-length effect was previously unknown and is not included in the NASA design criteria.[8] It is suggested in Ref. 7 that the authors of Ref. 5 could possibly offer an explanation for the greatly increased response amplitude for $L_N/d_N = 0.3$. This provided the incentive for the present investigation.

This paper revisits the aeroelastic stability problem of hammerhead payloads. The fluid-mechanical reason for the recently discovered critical cylinder length is discussed, along with its demonstrated detrimental effect on aeroelastic stability. Nose and nose-flare configuration effects are also discussed relative to their ability to cause flow separation and aeroelastic instability. A heretofore overlooked critical-cylinder-length effect on nose-cylinder-flare configurations is also discussed.

Background

The hammerhead payload problem first attracted attention in the early 1960s, when the Able IV payload was lost. It could be shown that the structural failure was a direct result of the longitudinal degree of freedom that the shallow boattail provided for shock-induced flow separation.[1,2,9] In order to eliminate this problem the NASA guidelines recommended a boattail angle greater than 20 deg.[8] The 35-deg boattail of the configuration in Fig. 1 obeys these guidelines.

The criterion of a steeper than 20-deg boattail is not always sufficient by itself, as is recognized in the NASA design criteria.[8] The Seasat payload shroud[10] was found to violate two of the three requirements for an aeroelastically stable hammerhead followed by a flare[8] (Fig. 4). In this case the proximity to the hammerhead boattail of the downstream interstage flare generated the bimodal flow separation shown in Fig. 5. That is, there exists a critical distance between the payload boattail and the downstream flare for which a small change of the payload attitude can cause the leeside boattail wake to merge suddenly with the flow separation forward of the flare. The resulting large discontinuous load aft of the forward node will result in an infinite aerodynamic undamping of the mode for infinitesimal-amplitude oscillations. As the oscillation amplitude increases, the aerodynamic undamping will diminish. Practically, limit-cycle oscillations will occur at an amplitude where the aerodynamic undamping is just balanced by the structural damping. The limit-cycle amplitude is usually so large as to cause structural failure. The solution in this case was simply to cover the entire upper stage and the payload with a large shroud with the same diameter as

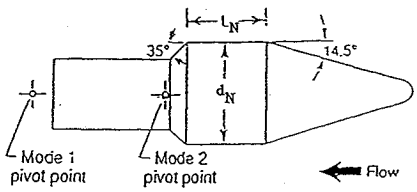

Fig. 1 Tested hammerhead geometries (Ref. 7).

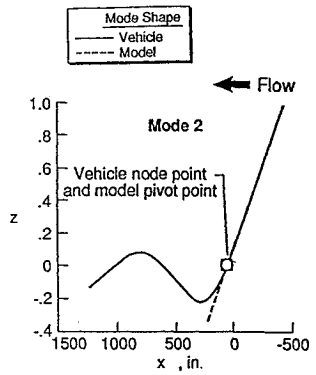

Fig. 2 Normalized mode shape for second bending mode (Ref. 7).

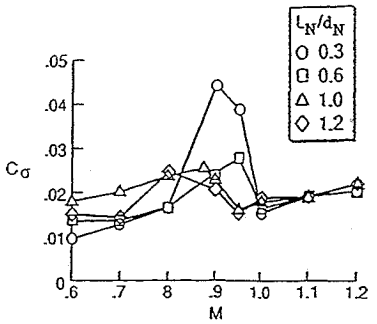

Fig. 3 Effect of L_N/d_N on buffet response for second mode (Ref. 7).

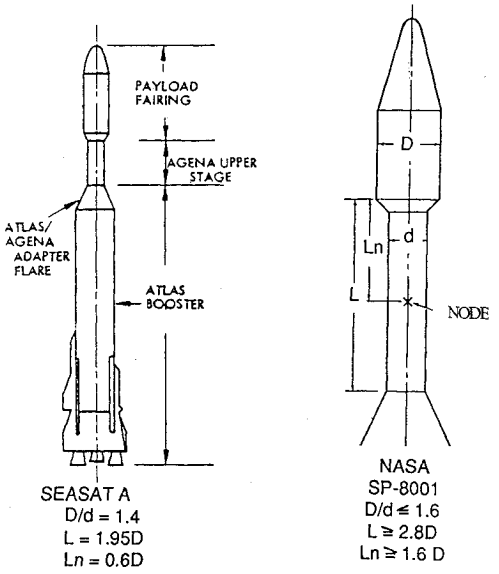

Fig. 4 Seasat-A configuration (Ref. 10).

the booster, thus eliminating the hammerhead and the potential for aeroelastic instability.[10] Incidentally, there was also a performance gain associated with the fix, since the drag of both the hammerhead base and the interstage flare were eliminated. This more than made up for the drag of the larger-diameter nose.

A similar sudden change of flow separation geometry has been observed in the wind tunnel on cone-cylinder bodies in a narrow, subsonic Mach number range[11,12] (Fig. 6). For cone angles 15 deg

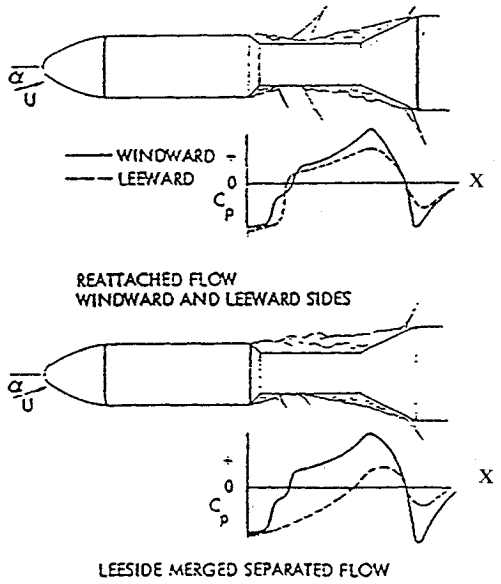

Fig. 5 Sketches of alternating flow conditions (Ref. 10).

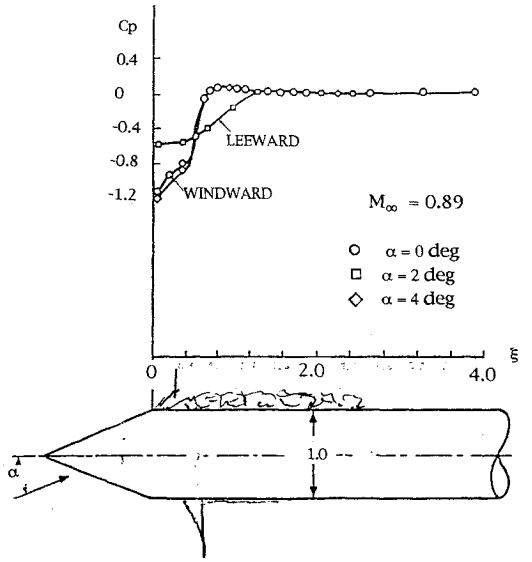

Fig. 6 Aerodynamic characteristics at M = 0.89 of a 20-deg cone-cylinder body with separated flow (Ref. 11).

$\leq \theta_c \leq 30$ deg a sudden change between the retarded and complete (nose-induced) types of flow separation occurred randomly, without any intentional external perturbations. The discontinuous load change was predicted to cause an aeroelastic undamping effect in good agreement with tests at $M = 0.9$ of the Saturn I launch vehicle with a Jupiter nose shroud.[6,13]

In both cases just described, the combined effects of accelerated flow[6] and convective time lag[4] result in an effective flowfield time lag that causes the discontinuous, statically stabilizing aerodynamic loading to be undamping. It is well documented that when a flowfield time lag is involved, loads that are statically stabilizing (returning the mode to its null position) are aerodynamically undamping.[1,2,4–6,10,14]

Discussion

Recent results[7] and a reexamination of earlier data[15–18] indicate that the current NASA criteria[8] are incomplete.

Hammerhead Cylinder

The NASA criteria for avoiding detrimental aeroelastic effects show no recognition of a criticality of the cylinder length on a hammerhead payload.[8] It appears that this is caused by a heretofore unrecognized flow phenomenon in which the hammerhead parameter L_N/d_N plays an important role. Apparently, the character of

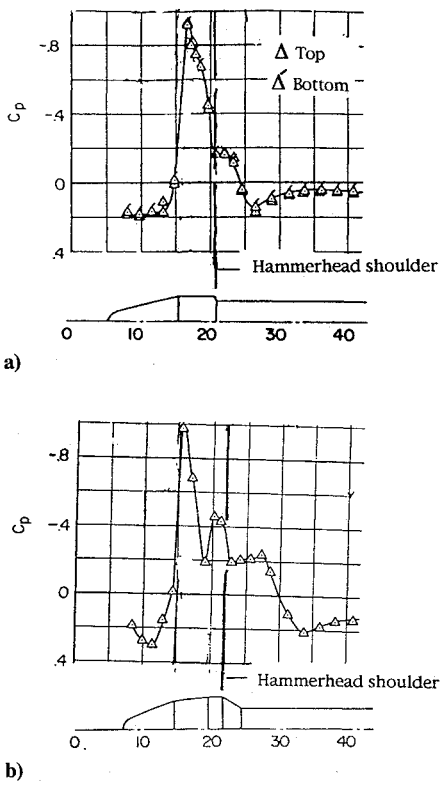

Fig. 7 Measured static pressure distributions on two hammerhead geometries at $M = 0.88$, $\alpha = 0$ (Ref. 14).

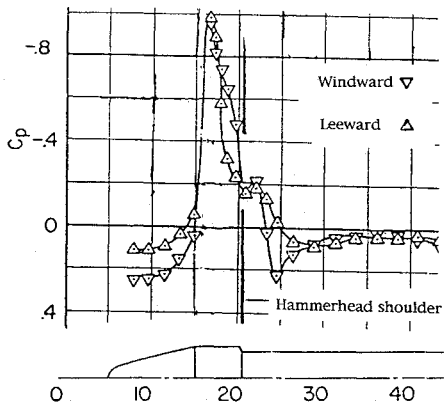

Fig. 8 Measured static pressure distributions on a hammerhead at $M = 0.88$, $\alpha = 4$ deg (Ref. 14).

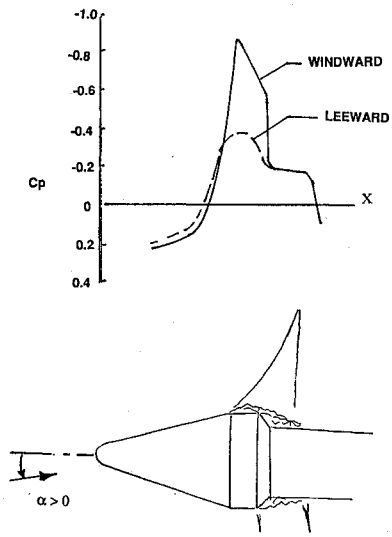

Fig. 9 Conceptual pressure distributions caused by sudden leeside flow separation for a 0.3-caliber hammerhead cylinder, $M = 0.89$.

the flow separation changes completely when this parameter is decreased to $L_N/d_N = 0.3$ and below, as there is a sudden increase in the buffet response at transonic speeds, $0.8 \leq M \leq 1.0$ (Fig. 3). (The wind tunnel data are from a partial-mode model where the mode shape forward of the first node is simulated.)

Data for similar hammerhead configurations indicate that, for a given Mach number, the base pressure is constant within experimental accuracy[14] (Fig. 7). Just before the base, a shock-induced pressure rise occurs. The same flow phenomenon is present at $\alpha = 4$ deg and $M = 0.88$, as can be seen in the pressure data of Fig. 8. The leeward pressure jump, caused by the terminal shock wave, is located forward of the windward pressure jump.[14] The forward movement of the leeside, shock-induced flow separation results from leeside boundary-layer thickening caused by crossflow effects. The level of the base pressure provides the boundary condition for the terminal normal shock. This is the pressure level downstream of the shock at a given Mach number regardless of the angle of attack or configuration (compare Figs. 7 and 8).

It is easy to see that when the cylinder is very short (0.3 calibers or less in this case), any forward movement of the leeside shock will produce an extremely large adverse pressure gradient, which interacts with the very low expansion pressures at the cone-cylinder shoulder. The resulting adverse pressure gradient is evidently too much for the cylinder boundary layer to handle, and the flow separation jumps to the cone-cylinder shoulder. The loss of leeside suction pressures at the shoulder (while they are preserved on the windward side) produces a very large, negative shoulder load (Fig. 9) forward of the hammerhead base. Since the node of the second mode is located aft of the base (Fig. 1), the negative, statically stabilizing force will be dynamically destabilizing or undamping,[4] resulting in the large buffeting loads shown in Fig. 3 for the $L_N/d_N = 0.3$ hammerhead cylinder.

The buffeting results[7] in Fig. 3 were obtained for a Reynolds number above 7.5×10^6 at the cone-cylinder shoulder.[19] The data used in Figs. 7 and 8 to explain the buffeting for $L_N/d_N = 0.3$ likewise had a solidly turbulent boundary layer[14] at the cone-cylinder shoulder. There was no indication of a leeside shock jump for $L_N/d_N \geq 1.0$, as it would have produced the maximum buffet response at $M = 0.9$. This is in contrast to the experimental results of Robertson and Chevalier for the 15-deg cone-cylinder.[11,12] However, their data were for a Reynolds number an order of magnitude lower and were therefore surely for laminar flow separation. The results for $L_N/d_N = 0.6$ in Fig. 3 indicate that there may be some feedback from the hammerhead base pressure also for this cylinder length. This agrees with results from high-Reynolds-number tests of this configuration,[14] which show the peak fluctuating pressure level aft of the cone-cylinder shoulder to occur at $M = 0.88$ for $\alpha = 4$ deg and at $M = 0.81$ for $\alpha = 0$. The fluctuating pressure level at $M = 0.89$ was found to be of negligible magnitude.

Nose and Nose-Cylinder-Flare Configurations

Recent heavy lift launch vehicle (HLLV) designs have tended toward very steep nose-cone angles to minimize weight (Fig. 10). These configurations violate the NASA guidelines for aeroelastic stability.[8] NASA recommended a nose-cone angle of less than 15 deg. This is to avoid transonic nose-induced flow separation. Figure 11 presents a typical pressure distribution for nose-induced separation measured on the Saturn I–Apollo booster with the escape rocket removed.[15] The data show a large negative load to occur aft of the cone-cylinder shoulder, followed by a positive load on the aft cylinder and flare. This produces a strong, stabilizing force couple. It is this force couple that, at high subsonic speeds, is responsible for the aft movement of the center of pressure for cone cylinders with 30- and 45-deg nose angles[16] (Fig. 12). Schlieren photographs confirm that this is caused by nose-induced flow separation (Fig. 13). It has long been recognized that dynamic instability occurs for rigid bodies dominated by nose-induced separated flow, primarily because of

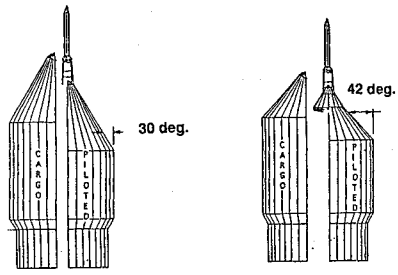

Cargo and piloted (with launch escape system) configurations

Fig. 10 HLLV noses.

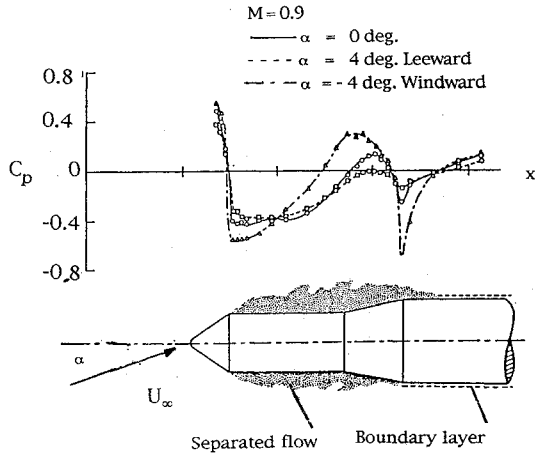

Fig. 11 Nose-induced separation pressures at $M = 0.9$ (Ref. 15).

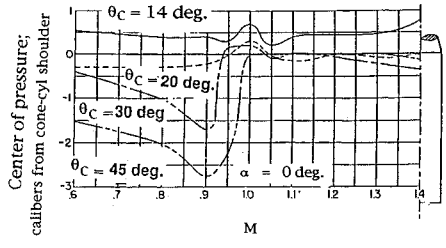

Fig. 12 Centers of pressures for cone-cylinder bodies, $\alpha = 0$ (Ref. 16).

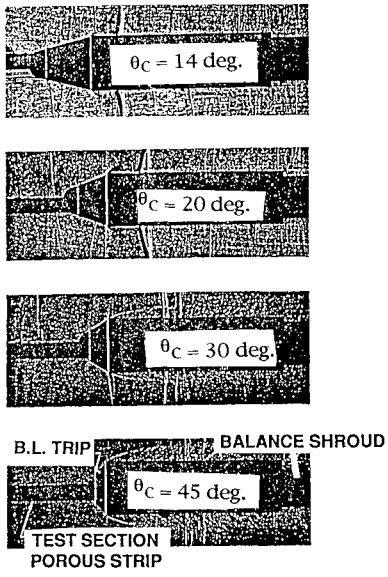

Fig. 13 Schlieren photographs for cone-cylinder bodies, $\alpha = 0$ (Ref. 16).

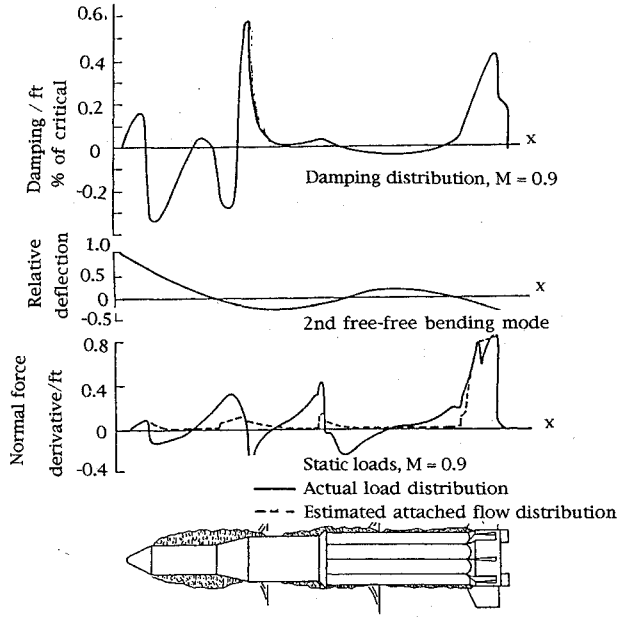

Fig. 14 Effects of nose-induced separation on the aeroelastic stability of the Saturn I–Apollo with escape rocket removed (Ref. 17).

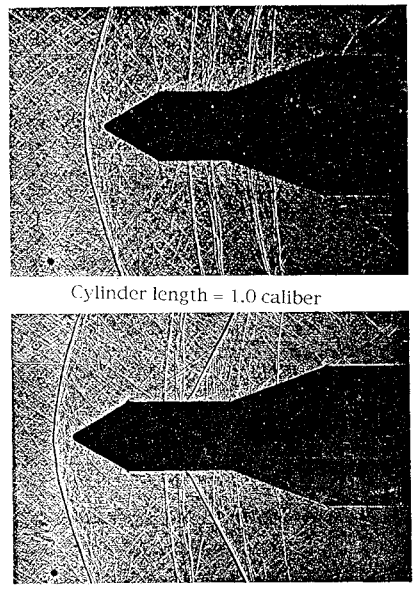

Fig. 15 Effect of cylinder length on flow-separation type at $M = 1.2$ (Ref. 18).

the flowfield time lag caused by the finite convection speed in the separated-flow region.[5,17] Likewise, nose-induced flow separation will cause aerodynamic undamping of the free-free bending modes of an elastic vehicle if a node occurs between the flow separation point, at the nose-cylinder shoulder, and the flow reattachment point. Thus, the Saturn I–Apollo booster showed large aerodynamic undamping components due to the nose-induced separation with the escape rocket removed[4] (Fig. 14).

While the escape rocket eliminated nose-induced separation for the Saturn-Apollo boosters, it is doubtful that it will do likewise for the HLLV. In the case of Saturn-Apollo, reattachment of the escape-rocket wake occurred very near the cone-cylinder shoulder, thereby altering the shoulder expansion. It is believed that the HLLV configurations will, unfortunately, experience reattachment well ahead of the shoulder, because of their larger noses, and the shoulder expansion will be unaffected by the escape rocket. Thus, the nose-induced flow separation will probably persist, as it does for the 30- and 45-deg noses in Figs. 12 and 13.

Nose-induced flow separation can occur at low supersonic speeds if an interstage flare is too close to the nose[18] (Fig. 15). Thus, if a

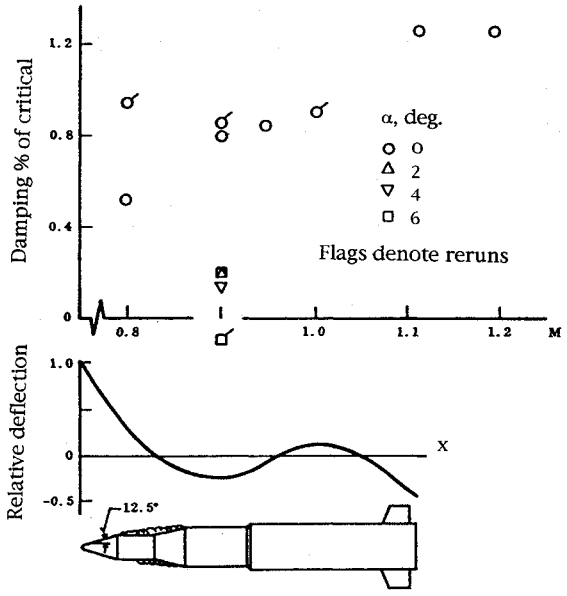

Fig. 16 Measured aerodynamic damping on an 8% elastic model of the Saturn I, Block II vehicle with a Jupiter nose shroud (Ref. 13).

node of the bending body occurs between the nose and the flare, aeroelastic instability will result, as it did[17] for the Saturn I–Apollo at $M = 0.9$ (Fig. 14). The presence of a downstream flare can also generate the adverse pressure gradient needed to cause sudden leeward flow separation for flow conditions where it would not otherwise occur. This is likely to have been the case for the Saturn I booster with a Jupiter nose shroud[6,13] (Fig. 16). Thus, both hammerhead and cone-cylinder-flare configurations experience critical-cylinder-length effects that are not recognized by the existing NASA guidelines.[8]

Conclusions

Recently renewed interest in large nonrecoverable launch vehicles has caused a re-examination of the NASA guidelines for aeroelastic stability. It is found that there are configurations that can threaten booster aeroelastic stability that presently are not recognized in the current NASA requirements. Specifically, critical-cylinder-length effects have been discovered for both hammerhead and cone-cylinder-flare payload configurations. The high buffeting loads measured for one critical hammerhead-cylinder length are the result of the upstream propagation of the hammerhead base pressures causing sudden nose-induced flow separation. Similarly, the adverse critical-cylinder-length effect for cone-cylinder-flare configurations is caused by upstream communication of the flare-induced pressure rise, resulting in a sudden change from regular to nose-induced flow separation through the increased adverse pressure gradient at the cone-cylinder shoulder.

Revisiting of the aeroelastic stability problem of unmanned launch vehicles has revealed that the current NASA guidelines need to be updated. More serious is the fact that even the existing NASA guidelines appear to have been ignored for many designs (Seasat A and HLLV). This is probably because there is not an appreciation of the catastrophic implications, namely, structural failure. This paper should serve to affirm the need to consider aeroelastic stability effects early in the design. With a thorough understanding of the flow phenomena, dynamically equivalent steady loads can be used in an analysis that, in the best case, eliminates the need for expensive redesign later in the development when aeroelastic problems are finally discovered. In the worst case it will reveal the reasons for a flight failure.

References

[1]Ericsson, L. E., Woods, P., and Chavez, J. N., "A Mechanism for Self-Excited Oscillations of 'Hammerhead' and Other Blunt-Nosed Missiles," *Proceedings of the 6th Symposium on Ballistic Missile and Aerospace Technology*, Vol. IV, Aug. 1961, pp. 69–88.

[2]Woods, P., and Ericsson, L. E., "Aeroelastic Consideration in a Slender Blunt-Nose, Multistage Rocket," *Aerospace Engineering*, Vol. 21, No. 5, 1962, pp. 42–51.

[3]Rainey, A. G., "Progress in the Launch-Vehicle Buffeting Problem," *Journal of Spacecraft and Rockets*, Vol. 2, No. 3, 1965, pp. 289–299.

[4]Ericsson, L. E., and Reding, J. P., "Analysis of Flow Separation Effects on the Dynamics of a Large Space Booster," *Journal of Spacecraft and Rockets*, Vol. 2, No. 4, 1965, pp. 481–490.

[5]Ericsson, L. E., and Reding, J. P., "Fluid Dynamics of Unsteady Separated Flow. Part I—Bodies of Revolution," *Progress in Aerospace Sciences*, Vol. 23, 1986, pp. 1–84.

[6]Ericsson, L. E., "Aeroelastic Instability Caused by Slender Payloads," *Journal of Spacecraft and Rockets*, Vol. 4, No. 1, 1967, pp. 65–73.

[7]Cole, S. R., and Henning, T. L., "Dynamic Response of a Hammer-Head Launch Vehicle Wind-Tunnel Model," *Journal of Spacecraft and Rockets*, Vol. 29, No. 3, 1992, pp. 379–385.

[8]Cole, S. R., and Henning, T. L., "NASA Space Vehicle Design Criteria, Volume II: Structures, Part B: Loads and Structural Dynamics, Chapter 3: Launch and Exit, Section I: Buffeting," NASA SP-8001, May 1964, revised Nov. 1970.

[9]Graham, F. J., and Butler, C. B., "Static Pressure Distribution on a 0.07 Scale Aerodynamic Model of the Atlas–Able IV at Free-Stream Mach Numbers from 0.50 to 1.60," Arnold Engineering Development Center, AEDC TN-60-128, Tullahoma, TN, July 1960.

[10]Reding, J. P., and Ericsson, L. E., "Effect of Aeroelastic Considerations on Seasat-A Payload Shroud Design," *Journal of Spacecraft and Rockets*, Vol. 18, No. 3, 1981, pp. 241–247.

[11]Robertson, J. E., "Unsteady Pressure Phenomena for Basic Missile Shapes at Transonic Speeds," AIAA Paper 64-3, Jan. 1964.

[12]Chevalier, H. L., and Robertson, J. E., "Pressure Fluctuations Resulting from Alternating Flow Separation and Attachment at Transonic Speeds," Arnold Engineering Development Center, AEDC TDR-63-204, Tullahoma, TN, Nov. 1963.

[13]Hanson, P. W., and Dogget, R. V., Jr., "Aerodynamic Damping and Buffet Response of an Aeroelastic Model of the Saturn I Block II Launch Vehicle," NASA TND-2713, March 1965.

[14]Coe, C. F., and Nute, J. B., "Steady and Fluctuating Pressures at Transonic Speeds on Hammerhead Launch Vehicles," NASA TM X-778, Dec. 1962.

[15]Reding, J. P., and Ericsson, L. E., "Static Loads on the Saturn I–Apollo Launch Vehicle," Lockheed Missiles and Space Co., Report LMSC/803185 (TM 53-40-143), Aug. 1963.

[16]Treon, S. L., "Effects of Nose-Cone Angle on the Transonic Aerodynamic Characteristics of a Blunt Cone-Cylinder Body Having a Cylindrical, Flared, or Blunt-Finned Afterbody," NASA TM X-582, Oct. 1961.

[17]Ericsson, L. E., and Reding, J. P., "Dynamics of Separated Flow over Blunt Bodies," NASA CR-76912, Dec. 1965.

[18]Guenther, R. A., and Reding, J. P., "Preliminary Experimental Investigation of Separated Flow Loads on Cone-Cylinder-Flare Bodies," Lockheed Missiles and Space Co., Report L-87-67-1, Feb. 1967.

[19]Cole, S. R., Private Communication, May 4, 1994.